ISSN Print: 2394-7500
ISSN Online: 2394-5869
Impact Factor (RJIF): 8.69
IJAR 2025; 11(10): 300-308
www.allresearchjournal.com
Received: 07-09-2025
Accepted: 11-10-2025

Yong-Song Choe
Faculty of Physical Engineering, Kim Chaek University of Technology, Pyongyang, Democratic People's Republic of Korea

Ji-Hyok Kim
Faculty of Physical Engineering, Kim Chaek University of Technology, Pyongyang, Democratic People's Republic of Korea

Myong-Son Hong
Faculty of Materials Science and Technology, Kim Chaek University of Technology, Pyongyang, Democratic People's Republic of Korea

Song-Hyok Kim
Faculty of Physical Engineering, Kim Chaek University of Technology, Pyongyang, Democratic People's Republic of Korea

Corresponding Author:
Ji-Hyok Kim
Faculty of Physical Engineering, Kim Chaek University of Technology, Pyongyang, Democratic People's Republic of Korea

Experimental Analysis of Ti(C, N) Based Nonmagnetic Cermet Using Ni(W) Solid Solution from Ammonium Metatungstate

Yong-Song Choe, Ji-Hyok Kim, Myong-Son Hong and Song-Hyok Kim

DOI: https://www.doi.org/10.22271/allresearch.2025.v11.i10d.12952

Abstract
An effective technique has been developed to prepare non-magnetic Ni(W) solid solutions using Ni and ammonium metatungstate (AMT) as raw materials and to be used as binders of non-magnetic Ti(C, N) based cermet. Powder particles using AMT as a source of tungsten have a higher contact area and activity between W and Ni. For this reason, the mutual diffusion between Ni and W and the solid-state reaction is promoted, and the amount of W diffusing in Ni is higher. The saturation magnetization values of Ni(W) solid solution powders using AMT as a source of W at suitable diffusion conditions (550 °C×2 h + 800 °C×2 h in H_2 atmosphere) were significantly lower compared to Ni(W) solid solution prepared using W and pure Ni. The degree of nonmagnetization of Ti(C, N) cermet with Ni(W) solid solution prepared from Ni and AMT as binder was superior to Ti(C, N) cermet with pure Ni as binder.

Keywords: Cermet, Ni(W) solid solution, nonmagnetic, powder metallurgy

1. Introduction
With the rapid development of science and technology, there is an increasing demand for functional cermets with various special physical properties and excellent mechanical properties, including non-magnetism [1-3].
The magnetism of cermet is mainly due to Co, Fe and Ni, which are used as binders, and Ni is the most favorable for the nonmagnetization of cermet [2, 4]. Therefore, it can be concluded that the proposed method of using non-magnetic Ni-based solid solutions as cermet binders for the non-magnetization of cermet is of significant value. When the mechanical alloying of the binder phase is promoted by metal atoms containing W in cermet, the interfacial energy between the alloy and ceramic phases is lowered and the wettability between the ceramic phase and the binder phase can be improved. Also, the solid-state strengthening of the binder phase plays an important role in enhancing the properties of Ti(C, N) based cermet.
Also, the solid-state strengthening of the binder phase plays an important role in enhancing the properties of Ti(C, N) based cermet. Secondly, the pre-solution treatment of cermet's binder not only increases the effect of the solid reinforcement but also promotes the dislocation enhancement in the binder phase [1]. Ni-W alloys are widely used in industry due to their superior mechanical, electrical and corrosion resistance compared to Ni, as effective candidates for hard chromium coatings, high temperature superconductors, and catalysts for H_2 release from alkaline solutions [5, 6], but few studies have been found on non-magnetic Ni-W alloys [5, 6]. Ni-W alloys can usually be prepared using electrodeposition [7, 8], mechanical alloying [9-13], and H_2 reduction of Ni-W oxides [14-16], etc. In the mechanical alloying process, Ni and W powders are commonly used as raw materials, and relatively high temperatures are required to form solid solutions.
AMT is the main raw material for the preparation of W powder, and ultrafine tungsten powder can be obtained by controlling the decomposition conditions of AMT, which is a condition that can promote the mutual diffusion between Ni and W [17].
From this point of view, we have prepared nonmagnetic Ni(W) solid solution powders by mechanical alloying and diffusion of Ni and AMT powders and compared the nonmagnetic degree of Ti(C, N) cermet with this Ni(W) solid solution powder and pure Ni as binder.

2. First principles research and experimental approaches

2.1. Modeling the Electronic Structure of Hardened Carbides by First Principle Studies and Calculation Method of Magnetic Strength

Since the magnetism of cemented carbides is closely related to the composition change of the Ni binder phase, the first-principles calculations were carried out to estimate the change in the saturation magnetization of WC-Ni cemented carbides with high W content for Ni binder phase, so that the high content of elements in the Ni binder phase can be predicted electronically. The initial structure of the alloy system was modeled using Material Studio 7.0. Since the atomic radii of Ni and W are not very different, they form substitution rather than interstitial structures. Hence, in the modeling of the system, we have constructed a supercell for the Ni structure, and then selected highly symmetrical sites to replace W.

The structure relaxation was then carried out with several structures with substitutions at different positions to select the most energetically stable substitution sites.

Next, the potential corresponding to each atomic species for the first-principles calculations was used for the ultra-soft potentials of Ni and W with the valence electrons of 3d84s2 and 5d46s2. To perform the optimization of the crystal structure, we used a plane wave cutting energy of 400 eV and a $8 \times 8 \times 8$ k-point mesh.

2.2. Experimental and measurement methods

Ni(W) solid solutions were prepared using AMT and pure W as sources of W, respectively.

The content of AMT (99% purity and 0.8 μm) was changed to 30.0, 33.8, 38.1, 41.6, and 46.2% (in terms of W, 20, 22, 25, 27, and 30%, respectively).

The powder mixing was carried out using mechanical alloying for 48 h in an XQM planetary ball mill, with a grinding ball set at a WC-Co-based cemented carbide, a ball/powder ratio of 7/1 and a rotational speed of 360 rpm.

The diffusion of Ni-AMT powder was first carried out at 550 °C for 2 h under H_2 atmosphere and then again at 750 °C or 800 °C for 2 h, respectively.

When pure W was used instead of AMT, Ni (99.9%, 36 μm) and W (99.9%, 18 μm) powders were prepared by mixing at a weight ratio of 80/20, and the mechanical alloying conditions were set equal to those using AMT.

Diffusion was carried out for 2 h at 750 °C or 800 °C in H_2 atmosphere, respectively.

Next, Ni(W) solid solution and pure Ni prepared in the composition of Ni-30%AMT(25% in W) were used as binders to prepare Ti(C, N)-15% Ni(W) and Ti(C, N)-15%Ni alloys, respectively.

Sintering was carried out in a vacuum sintering furnace at 1460 °C and a holding time of 40 min.

The microstructure of the mechanically alloyed powders and the diffusive powders was observed by JSM-7001F type thermal field emission scanning electron microscopy (SEM) and the particle size of the powder was measured by a LA-920 type laser dispersive particle size distribution meter.

And the phase composition of the mechanically alloyed and diffusive powders was carried out using a Smart lab-type polycrystalline X-ray diffract meter (XRD), using a Cu K-ray.

Also, the high-dose of W on the Ni lattice was calculated by measuring the diffraction angle of the (111) crystal plane of the Ni(W) phase and using Eq. (1) as shown in [18].

$$X_W = -7.5208 + 2.13429A_{Ni\text{-}W}, (1)$$

where X_W is the atomic fraction of W in Ni, and A_{Ni-W} is the lattice parameter.

The saturation magnetization of the mechanically alloyed and diffusive powders was measured using a Lake Shore model vibrating magnetization measuring device and corrected using pure Ni as reference material.

Next, the mass of the sample was measured, the sample was fixed on a non-magnetic holder, an external magnetic field of 800 kA/m was applied, and six samples were selected for each test condition to measure the saturation magnetization and calculate the average value.

3. Results and discussion

3.1. Changes in Ni lattice structure and electronic structure with high W dose

Fig. 1 shows the relaxed structure of Ni(W) solid solution when the high doses of W are 5.0, 7.0 and 10.0 atomic%, respectively.

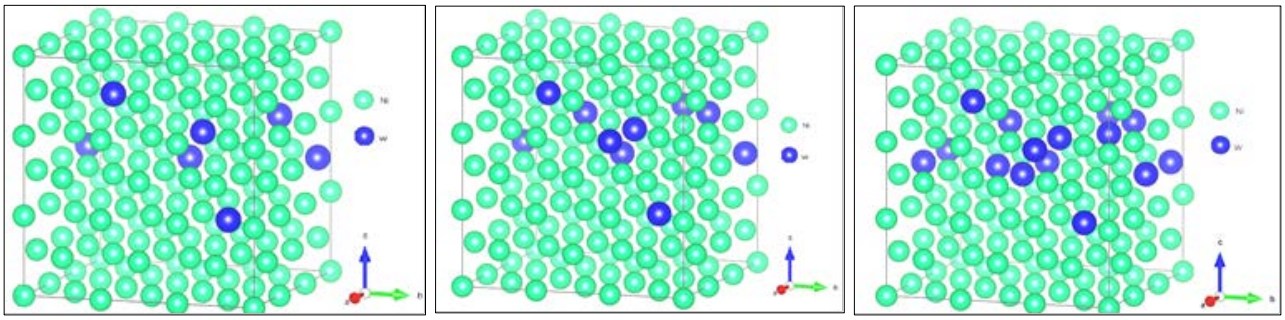

(a) (b) (c)

Fig 1: Relaxed structure of Ni(W) solid solution with different W solid solubility a: 5.0at% b: 7.0at% c: 10.0at%

Considering the magnetic change of Ni when W is employed in pure Ni, we have. This indicates that Ni is a typical ferromagnetic.

On the other hand, the electron configuration of Ni has an unfilled d orbital of 3d84S2, which is ferromagnetic by the d-orbital electrons, as can be seen from the partial density of states shown in Fig.2 (a).

For s- or p-orbital electrons, the magnitude of the spin density of states is small and nearly symmetric, so that they contribute little to the magnetization and the spin magnetic moment value is less than 1.

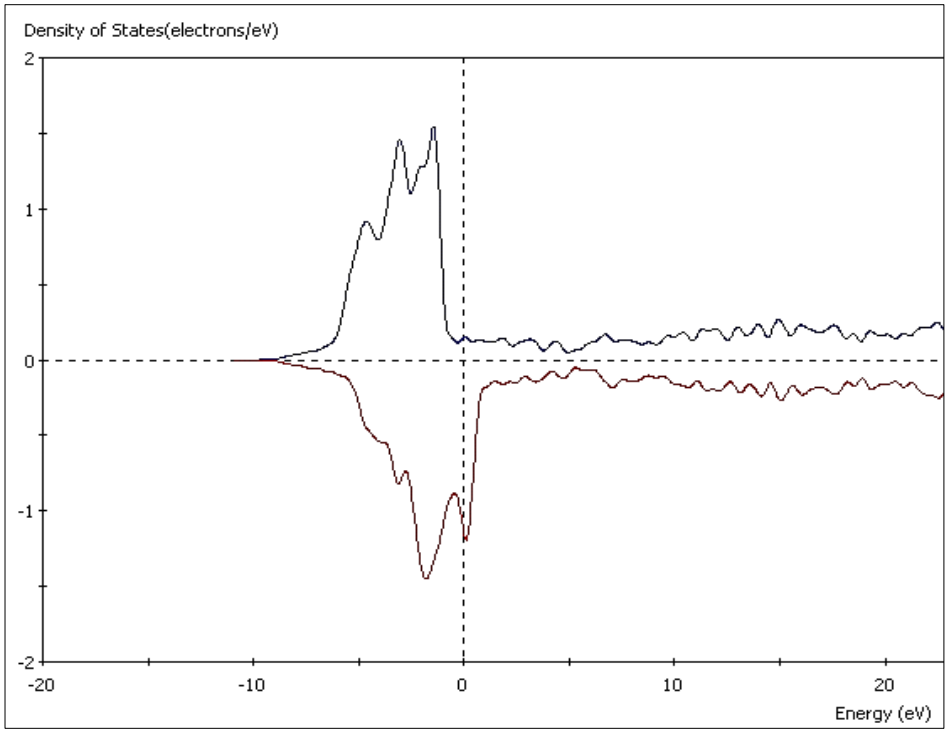

(a)

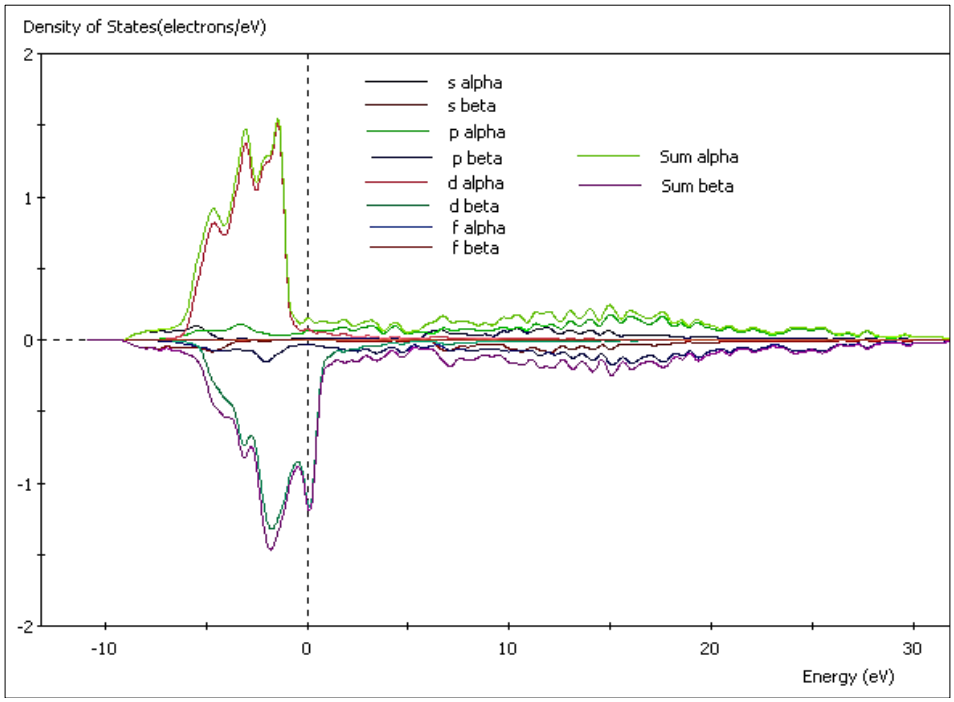

(b)

Fig 2: TDOS and PDOS of pure Ni (a) TDOS (b) PDOS

In general, it seems that the magnetic moment of Ni from the electron configuration 3d84S2 will be 5-3 = 2 μB (Bohr magneton) for the d orbital, but not necessarily.

When transition metal atoms form metal crystals, the magnitude of the magnetic moment is not determined by the algebraic sum of the spin magnetic moments of the electrons in the 3d and 4s states, but rather by the arrangement of electrons in the outermost electron layer, which is different from that in the presence of metal atoms, the rearrangement occurs. That is, the value of the spin magnetic moment will be different.

The orbital occupancy of electrons with spin is shown in Table 1.

Table 1: Electron density in the optimized state

Specimen	Ion	s	p	d	f	Total
Ni	1	0.56	0.74	8.7	0.00	10.00

As shown in Table 1, the electronic contribution of d orbitals, which has a large effect on the magnetism, is 8.7, which is larger than the initial 8, indicating that more electrons contribute to d orbitals, whereas the contribution to s orbitals becomes smaller.

However, the addition of tungsten completely alters the magnetic properties as shown in Fig.3.

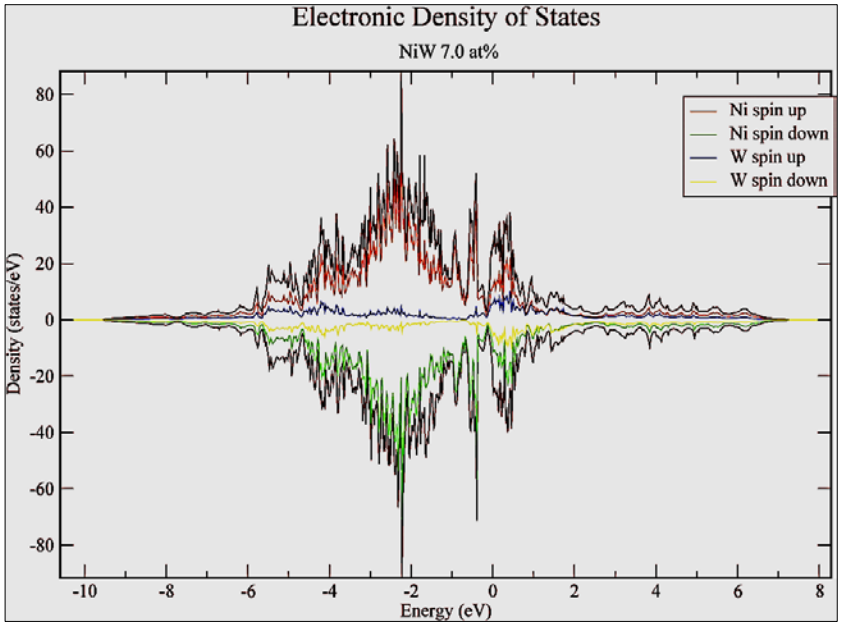

(a)

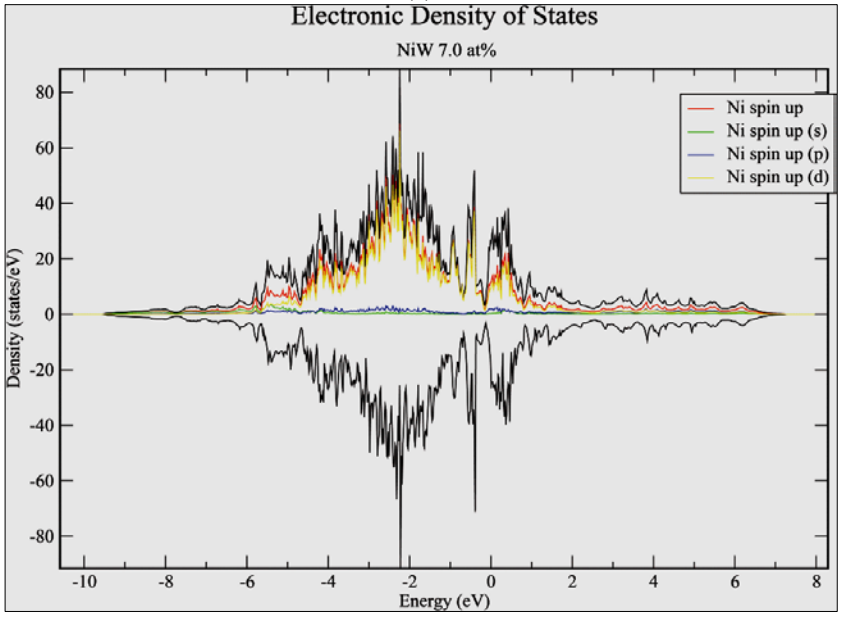

(b)

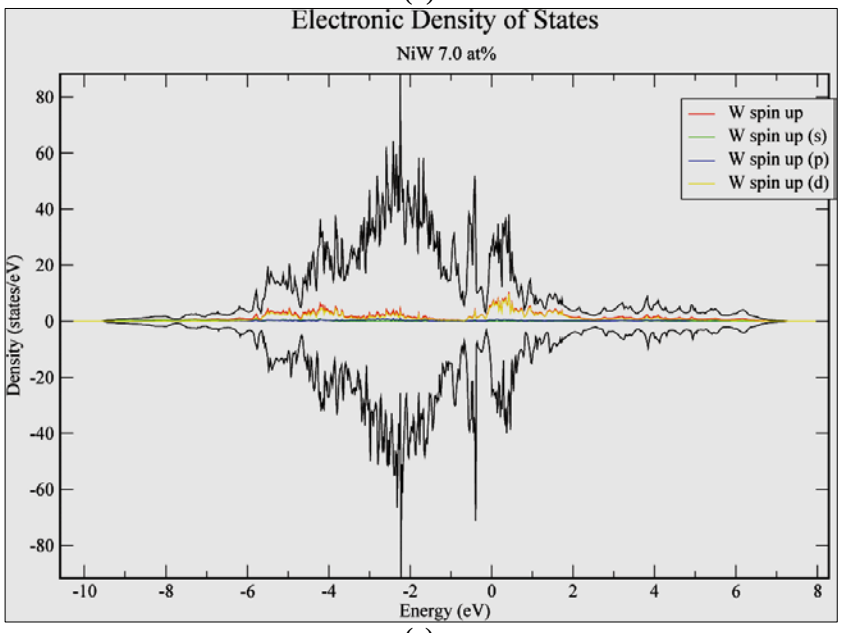

(c)

Fig 3: TDOS and PDOS of Ni(7.0at%W)

Thus, the electronic shell structure of electrons within an atom will also be altered, and the bonding mechanism between atoms will be significantly different from that of pure Ni.

As a result, the density of states of Ni, which is completely spin-polarized, becomes almost symmetrical, so that the ferromagnetism disappears and the magnetization becomes very small. In particular, weak magnetization by the 5d electrons of tungsten is observed, indicating that even when a small amount of tungsten is employed, the local potential field in Ni can be completely changed, which has a great influence on the electronic configuration and, consequently, a large change in magnetic properties.

At that time, the magnetic susceptibility of system is calculated as follows:

The magnetization is given by the sum of the magnetic moments (or magnetic efficiencies) per unit volume.

$$\hbar = \frac{h}{2\pi} = 1.06\times10^{-34}\,\mathrm{J\cdot s} \tag{2}$$

where h: Planck's Constant($6.626\times10^{-34}\,\mathrm{J\cdot s}$), e: Elementary Charge(1.6×10^{-19}C), m_e: Mass of Electron(9.1×10^{-31}kg)

In general, paramagnetism occurs at high temperatures, where at high temperatures the magnetic moments are oriented randomly due to thermal vibrations, and the magnetic moments of the material are totally zero.

At low temperatures, the system transitions to a state with long-range magnetic order, which is caused by the exchange interaction between magnetic moments, and generally occurs at temperatures comparable to the strength of the interaction between the neighboring moments.

In ferromagnets, long-range magnetic ordering is manifested as spontaneous magnetization. Thus, magnetization exists even in the absence of an external magnetic field.

To calculate the magnetization, we must apply the spin density functional theory (SDFT) with respect to the spin of the electron. The magnetization density is given by $m_z(\boldsymbol{r}) = n_\uparrow(\boldsymbol{r}) - n_\downarrow(\boldsymbol{r})$, and the zeta function has a value between -1 and 1. These quantities are zero at all points in space in the case of non-magnets, and in the case of magnets, they are integrated in the unit cell to determine the total magnetization.

To consider the distribution of energy eigenvalues in all directions of magnetization, the spin-resolved density of states was calculated as follows

First, we calculate the density of states for all spins separately, then integrate the density of states to calculate the number of electrons in each spin direction. In magnets, the number of electrons varies with the spin direction, and the number of spins with large electron numbers is called the primary spin, the spins with small electron numbers are called the minority spins, and the units of magnetization obtained by integrating over the unit cell are μ_B (Bohr magneton).

The calculation of the saturation magnetization was carried out using Eq. (3).

$$M_S = \mu_0 M = \mu_0 m / V_0 \tag{3}$$

where M_S is Magnetic saturation in [T], μ_0 is Initial permeability in [H/m], M is Magnetic moment per unit volume in [A/m], m is Magnetic moment per unit cell in [A·m^2] and V_0 is Volume of unit cell in [m^3].

The calculated results of the saturation magnetization versus the W loading of Ni are shown in Fig. 4 as follows.

0 at%: $M_s = 6114\times10^{-4}\,\mathrm{T}$ [21]

5.0 at % (15%):
$$M_s = \frac{4\pi\times10^{-7}\times4.422103\times9.274\times10^{-24}}{(10.19583\times10^{-10})^3} = 486.1\times10^{-4}\,\mathrm{T}$$

7.0 at % (20%):
$$M_s = \frac{4\pi\times10^{-7}\times2.478441\times9.274\times10^{-24}}{(10.21057\times10^{-10})^3} = 271.2\times10^{-4}\,\mathrm{T}$$

10.0 at % (25%):
$$M_s = \frac{4\pi\times10^{-7}\times2.11132\times9.274\times10^{-24}}{(10.2339\times10^{-10})^3} = 229.5\times10^{-4}\,\mathrm{T}$$

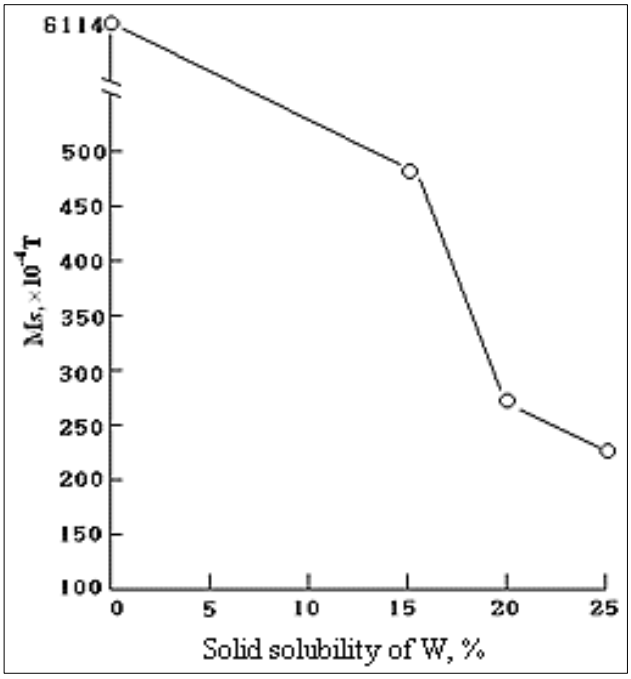

Fig 4: Variation of the magnetic saturation of Ni(W) solid solution with solid solubility of W

As can be seen, the saturation magnetization of Ni decreases rapidly with increasing the high dosage of W in Ni, with 271.2×10^{-4} T at 20% high dosage, and the saturation magnetization of pure Ni decreases by about 1/25 compared to 6114×10^{-4} T.

It can be seen that the solvation effect of Won the nonmagnetization of Ni is large and its effectiveness is obvious, with the high solid content of Ni from 20 to 25%, and the reason for the non-magnetization of Ni by the solid solution of W is due to the decrease of the spin magnetic moment of Ni.

Therefore, it is important to determine the carbon content to dissolve more than 20% W in Ni in practical non-magnetic Ti(C, N)-Ni cermets.

3.2. Effect of composition and diffusion conditions on the formation and magnetic properties of Ni(W) solid solution

The diffusion of Ni-30%AMT and Ni-15%W mechanical alloying powders was carried out and their SEM micrographs and grain sizes are shown in Figs. 2 and 5, respectively.

The diffusion of the mechanical alloying powder of Ni-AMT was first carried out at 550 °C for 2 h and then in an H_2 atmosphere at 800 °C for 2 h.

Meanwhile, the diffusion of the mechanical alloying powder of Ni-W was carried out in an H_2 atmosphere at 800 °C for 2 h.

The results showed that the Ni-AMT diffusive powder was finer than the diffusive powder of Ni-W.

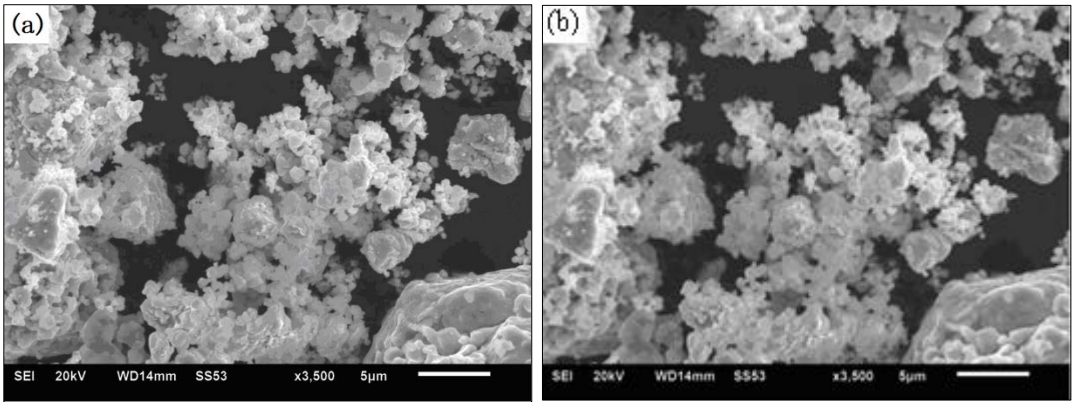

(a) Ni-30 wt. % AMT diffused powder; (b) Ni-20 wt. % W diffused powder

Fig 5: SEM graphics of the diffused powders.

Table 2: Particle size of the powders

The kinds of powders	Median grain size (μm)	Mean grain size (μm)
Ni-20 wt.% W MA'd powder	3.70	4.80
Ni-20 wt.% W diffused powder	12.55	13.09
Ni-30 wt.% AMT MA'd powder	1.94	2.60
Ni-30 wt.% AMT diffused powder	6.77	7.41

The X-ray diffraction curves of Ni(W) powders prepared at different diffusion temperatures are shown in Fig. 6, and it can be seen that all diffraction peaks of the diffusing powder belong to the solid solution of Ni(W).

And the shift of diffraction peaks belonging to Ni was the result of the incorporation of W into the Ni lattice, and it was found that the diffraction peaks of the diffusing powder of Ni-AMT were shifted more than those of the diffusing powder of Ni-W.

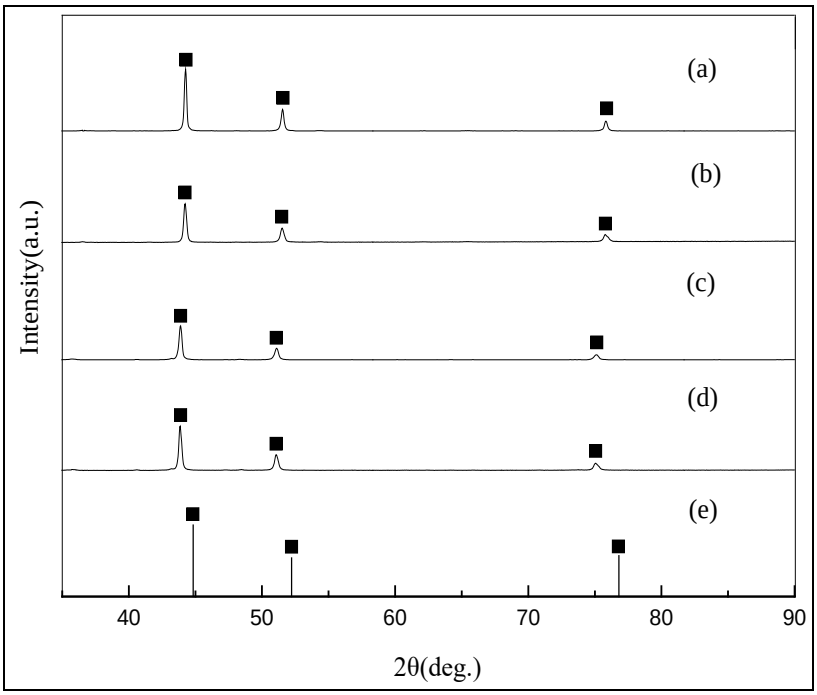

Fig 6: X-ray diffraction (XRD) patterns of the diffused powders.

Ni-15%W (700℃×2h), (b) Ni-15%W (800℃×2h), (c) Ni-30%AMT (550℃×2h→700℃×2h), (d) Ni-30%AMT (550℃×2h→800℃×2h), (e) Standard PDF card information of nickel (JCPDS 04-0850). (■) Ni solid solution phase.

Next, the variation of the high-dose and saturated magnetization of W in Ni of the solid solution powders of Ni(W) prepared under different diffusion conditions is presented in Table 3.

Table 3: The amount of W in Ni and magnetic saturation (Ms) of the powders

The kinds of powder	Amount of W in Ni (wt. %)	Ms (emu/g)
Ni-30 wt.% AMT (550℃×2h→750℃×2 h)	17.38	1.82
Ni-30 wt.% AMT (550℃×2h→800℃×2h)	17.97	0.03
Ni-20 wt.% W (750℃×2 h)	15.78	5.00
Ni-20 wt.% W (800℃×2 h)	16.30	3.92

As shown in Table 3, the high dosage of W in Ni was higher when AMT was used as a source of W compared to pure W at the same reduction temperature.

And when the diffusion temperature was increased from 750 to 800 °C, the high dosage of Ni-30%AMT diffusing powder increased from 17.38% to 17.97%, and the saturation magnetization decreased from 1.82 emu/g to 0.03 emu/g.

On the other hand, when the diffusion temperature was increased from 750 to 800 °C, the high capacity of Ni-15%W of the diffusion powder increased from 15.78% to 16.30%, and the saturation magnetization decreased from 5.00 emu/g to 3.92 emu/g.

From the above results, it can be seen that the higher the diffusion temperature, the lower the saturation magnetization of the diffusion powders, while at the same diffusion temperature, the saturation magnetization of the diffusion powders of Ni-AMT is lower than that of the diffusion powders of Ni-W.

3.3 Effect of high dosage of W in Ni on the saturation magnetization

Fig. 7 shows the X-ray diffraction curves of Ni(W) solid solution powders with the addition of AMT, and regardless of the content of AMT, only the diffraction peaks belong to Ni(W) solid solution.

Also, with the increase of the addition of AMT, the diffraction peak of Ni(W) of the diffusing powders shifted to the left, which could be a result of the increase of the high content of W on the Ni lattice.

The variation of the high-capacity and saturated magnetization of W in Ni of Ni (W) solid solution powders with different AMT contents is shown in Fig. 7.

It can be seen that with the increase of the content of AMT, the high dosage of W in Ni (W) solid solution powders increased from 17.97% to 24.00%, and the saturation magnetization decreased from 0.03 emu/g to 3.8 10-5 emu/g.

Thus, when the high dosage of W in Ni was more than 21%, the saturation magnetization of Ni(W) solid solution powder was almost zero.

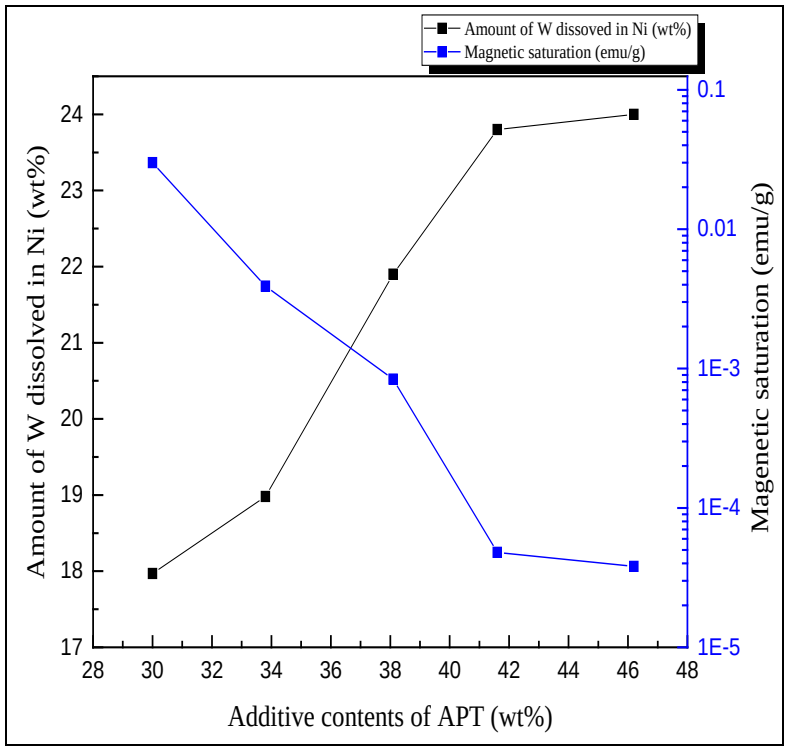

Fig 7: The variation of W solubility amounts in Ni and the magnetic saturation (Ms) of Ni(W) solid solution powders with AMT additive contents.

This is consistent with the fact that the high solid content of W in Ni is more than 18% as indicated by the Ni-W binary alloy phase diagram [3], the magnetostatics of Ni are lowered to room temperature and Ni becomes nonmagnetic.

And the calculated high-dose values of W in Ni-AMT and Ni-W diffusing powders decreased compared to the initial W content, which could be attributed to the thermal amorphization of the powders by mechanical alloying reported in [13-16].

3.4 Magnetic changes of sintered samples

The high-capacity and saturated magnetization of the Ni alloys (W, Ti) and Ti(C, N)-15%Ni(W) alloys prepared using AMT as the source of W and pure Ni as binders, respectively, were measured, and shown in Table 3, the high-capacity of the Ni heavy alloys of Ti(C, N)-15%Ni(W) alloys was much lower compared to Ti(C, N)-15%Ni(W) alloys, and the saturation strength was lower compared to Ti(N, 15%)-Ni alloys, respectively.

Table 3: Amount of W in Ni lattice and magnetic saturation of the alloys.

The kinds of alloy	Amount of W in Ni lattice (wt. %)	Magnetic saturation (emu/g)
Ti(C, N)-15%Ni(W)	26.96	2.8×10^{-4}
Ti(C, N)-15%Ni	24.07	0.84

This is because the incorporation of non-magnetic particles such as W and Ti into Ni reduces the interaction of magnetic atoms by reducing the proportion of Ni magnetic atoms [17]. Thus, using non-magnetic Ni (W) solid solution as a cementitious binder of cermet is an effective way to prepare non-magnetic cermet.

Conclusion

Ni and ammonium metatungstate (AMT) were used as raw materials to prepare non-magnetic Ni(W) solid solutions through mechanical alloying and diffusion.

1) The saturation magnetization (Ms) of Ni(W) solid solution powders prepared using AMT as a source of W under identical preparation conditions was lower than that using W powder. Powders prepared using AMT as a source of W were more finely grained with higher activity, which could be a result of the higher solid-state reaction of W in Ni and the increased high dosage of W in Ni by the interdiffusion between Ni and W.
2) As the high dosage of W in Ni increased, the saturation magnetization of Ni(W) solid solution decreased, and mechanical alloying and diffusion of Ni and AMT were effective methods for preparing non-magnetic Ni(W) solid solution powders.

The diffusion conditions for preparing the non-magnetic Ni(W) solid solution powders using Ni and AMT were 550 °C×2 h + 800 °C×2 h in H_2, when the high solid content of W in Ni was over 18%, and the obtained Ni(W) solid solution powders were almost nonmagnetic.

3) The high content of the alloying elements in Ni of Ti(C, N)-15%Ni(W) alloy using the obtained non-magnetic Ni(W) solid solution powder as binder was higher compared to that of Ti(C, N)-15%Ni alloy using pure Ni as binder, thereby resulting in a lower saturation magnetization of the alloy and thus a non-magnetization.

Statements and Declarations

Funding

The authors declare that no funds, grants, or other support were received during the preparation of this manuscript.

Competing Interests
The authors have no relevant financial or non-financial interests to disclose.

Author Contributions
All authors contributed to the study conception, methodology and software. Visualization, formal analysis and writing-original draft were performed by Yong-Song Choe. Validation and writing- original draft were performed by Ji-Hyok Kim. Validation and writing-review & edition were performed by Myong-Son Hong. Data collection is performed by Song-Hyok Kim. All authors read and agreed the final manuscript.

Data Availability
The datasets analysed during the current study are available from the corresponding author on reasonable request.

References

1. Zhang M, Yang Q, *et al*. Effect of binder on corrosion resistance of Ti(C, N)-based cermet. Rare Metal Materials and Engineering. 2022;51(11):23-28.
2. Yan Y. Method of preparation of cermet raw powder and cermet. CN108220734 B. 2020 Oct 16.
3. Duan H, *et al*. Effect of Ni content on high temperature oxidation resistance of TiN-Ni-based cermet. Rare Metal Materials and Engineering. 2020;49(2):51-54.
4. Eliaz N, Sridhar TM, *et al*. Synthesis and characterization of nickel-tungsten alloys by electrodeposition. Electrochim Acta. 2005;50:2893-2904.
5. Sriraman KR, Raman SGS, *et al*. Synthesis and evaluation of hardness and sliding wear resistance of electrodeposited nanocrystalline Ni-W alloys. Mater Sci Eng A. 2006;418:303-311.
6. Borgia C, Scharowsky T, *et al*. A combinatorial study on the influence of elemental composition and heat treatment on the phase composition, microstructure and mechanical properties of Ni-W alloy thin films. Acta Mater. 2011;59:386-399.
7. Alimadadi H, Ahmadi M, Aliofkhazraei M, *et al*. Corrosion properties of electrodeposited nanocrystalline and amorphous patterned Ni-W alloy. Mater Des. 2009;30:1356-1361.
8. Aning AO, Wang Z, *et al*. Tungsten solution kinetics and amorphization of nickel in mechanically alloyed Ni-W alloys. Acta Metall Mater. 1993;41:165-174.
9. Mi S, Courtney TH, *et al*. Processing, structure and properties of Ni-W alloys fabricated by mechanical alloying and hot isostatic pressing. Scr Mater. 1998;38:637-644.
10. Streletskii AN, *et al*. Kinetic, chemical and mechanical factors affecting mechanical alloying of Ni-bcc transition metal mixtures. Mater Sci Eng A. 2000;282:213-222.
11. Nasu T, Sakurai M, Kamiyama T, Usuki T, Uemura O, Tokimitsu K, *et al*. Structural comparison of M-W (M = Fe, Ni) alloys produced by electrodeposition and mechanical alloying. Mater Sci Eng A. 2004;375:163-170.
12. Genç A, Öveçoğlu ML, *et al*. Fabrication and characterization of Ni-W solid solution alloys via mechanical alloying and pressureless sintering. Mater Des. 2012;42:495-504.
13. Mentus S, Majstorovic DM, *et al*. Reduction of NiO-WO_3 oxide mixtures synthesized by gel-combustion technique: A route to Ni-W alloys. Mater Sci Forum. 2005;494:345-352.
14. Mentus S, Tomic-Tucakovic B, *et al*. Gel-combustion synthesis of NiO-MoO_3 mixtures and their reduction to Ni-Mo alloys. Mater Chem Phys. 2008;112:254-261.
15. Genç A, Öveçoğlu ML, *et al*. Characterization of Ni-W solid solution alloy powders and sintered compacts synthesized via mechanically activated hydrogen reduction of NiO-WO_3 mixtures. Mater Int. 2013;19(4):813-819.
16. Wan LS. *Tungsten*. Beijing: Metallurgical Industry Press; 2010. p. 297.
17. Juskenas R, Valsiunas I, *et al*. On the state of W in electrodeposited Ni-W alloys. Electrochim Acta. 2009;54:2616-2620.
18. Maweja K, Phasha MJ, *et al*. Thermal stability and magnetic saturation of annealed nickel-tungsten and tungsten milled powders. Int J Refract Met Hard Mater. 2012;30:78-84.
19. Schulz R, Trudeau ML, *et al*. The contribution of strain and plastic deformations to the amorphization reaction of Ni-Zr alloys by mechanical alloying. Mater Sci Eng A. 1991;134:1354-1362.